ISSN: 0976-9102 (ONLINE)
DOI: 10.21917/ijivp.2022.0378

DETAIL PRESERVED DENOISING ALGORITHM VIA PATCH BASED EDGE SIMILARITY INDEX AND JOINT BILATERAL FILTER

Dayana David
Department of Department of Agricultural Statistics, Kerala Agricultural University, India

Abstract

Denoising algorithms are getting more attention in these days because they play a vital role in other applications of image processing. As details structures are the important information of Human Visual System, its preservation in denoised image is highly demanding one. A two-step denoising algorithm based on Patch based Edge Similarity Index and Joint Bilateral Filter algorithm proposed in this paper, preserves the edge structures and produce visually pleasant denoised image. Edge Similarity Index (ESI) proposed in the paper group patches according to their similarity in orientation and hence preserve the detail feature. The optimally grouped patches transferred to Principal Component Analysis (PCA) domain and the proposed noise suppression method eliminates the noisy component. Adaptive soft thresholding noise suppression method suppress the noise based on local noise estimation. Noise estimation in local level helps to estimate the noise accurately where noise affected differently in regions of a scene. Strong noises residuals may exist after first step, the denoised image in the first step further processed by a Joint Bilateral Filter for producing visually pleasant denoised image. Experimental results shown that proposed denoising algorithm achieves comparable detail preserving performance in terms of visual analysis and quantitative analysis over other state of art method.

Keywords:

Fixed Patch, Variable Patch, Denoising Patch, Edge Similarity Index, Joint Bilateral Filter

1. INTRODUCTION

The presence of noise deteriorates the visual quality of the images. Hence, image denoising is an essential pre-processing steps in image processing applications such as detection, classification, and recognition which requires high quality input images. As edges and textures are the important features of the image, the denoising algorithms which retains these details are the need of the hour. Additive White Gaussian Noise is the most common noise that deteriorate the observations. Gaussian Noise is an independent and identically distributed noise with zero mean and non-zero variance. The proposed denoising algorithm removes the Gaussian noise and produces artifact free, detail preserving denoised images.

Based on the domain, denoising algorithms are categorized in two types: denoising algorithms in spatial domain and denoising algorithms in transformed domain. Classical filters like Bilinear filter [1], Anisotropic diffusion filter [2], and Kernel Regression filter [3] works in spatial domain for removing noise and proposing denoising images.

The invention of non-local mean NLM approaches [4] and its improvement [5] brings a new strategy for removing the noise components. In NLM methods the similar patches are identified non-locally from image and weighted average performed by computing the Euclidean distance between center patch and similar patch. Distance measurement in NLM for identifying the similarity does not work well if noise level is high. Another line of research, BM3D, [6] also provides a basement for several denoising algorithms. It achieves superior results by applying a three-dimensional transform on a three-dimensional patch block. BM3D algorithm is time consuming even if it produces better result. The Dictionary-based [7] and patch-based techniques [8] are also exist in literature for denoising images. Even though these algorithms work well, they are not good at retaining details and avoiding artifacts simultaneously.

Since it is easy to separate noisy pixels and noise free pixels in transformed domain, the transform domains like Discrete Cosine Transform, Wavelet Transform domain, and Principal Component Analysis (PCA) domains were widely used in literature for denoising the images. As noise exists in high frequency coefficients in wavelet domain, the filtering of these components produces denoised image. In wavelet based denoising methods the noise has been removed by modifying or removing wavelet coefficient [9-10]. The success of the techniques lies in the accurate estimation of real images from noisy components. As fixed wavelet basis are unable to preserve local structures, Wavelet based denoising algorithm introduces many visual artifacts in denoised images. The DCT based noise removal algorithms [11] uses hard thresholding on DCT coefficients for removing noise. The limitations of denoising in these domains is the limitation in inadequate representation of spatial structures.

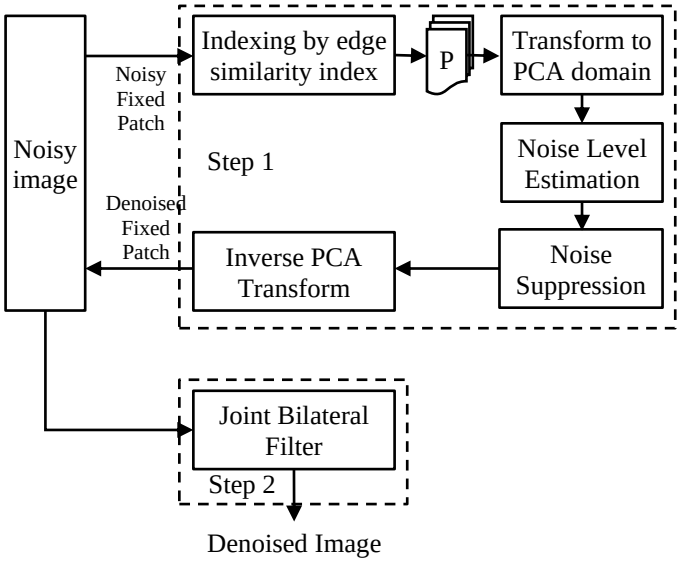

Fig.1. Architecture of the Proposed Method

Comparing to other transform domain, the PCA domain can represent structural features in efficient way. In image processing, PCA is widely used for dimensionality reduction and pattern recognition [12]. In PCA transformed dataset most important components are separated from least important components.

Hence, by retaining most important components, noise and trivial information can be easily removed in PCA domain. PCA based algorithm [13]-[15] provides a new era for denoising algorithms. LPG-PCA algorithm [13] remove the noise component by grouping pixels and, noise has been removed through method linear minimum mean-square error (LMMSE) method in PCA domain. Adaptive PCA based denoising algorithm [15] employs the local features while removing noise. While applying PCA transformation directly to the image the noisy components mislead the denoising process and produces an artifact in denoised image. The proposed method eliminates this drawback by indexing the image patches according to the detailed information prior to PCA transformation. By giving more emphasis to features like edges and textures, proposed method produces details preserved denoised image.

The proposed method removes noisy observations in two steps. In first step, the denoising performed in transform domain and in second step image again denoised in spatial domain for removing rest of the noise components. An Edge Similarity Index (ESI) is proposed for grouping optimal patches with similar orientation and arranged as stacked patch matrix. The advantage of categorizing patches based on detail feature is that edges are less affected by noise and hence, the similar patches can identify efficiently in the presence of noise. Since noise level is unknown, a local noise estimation is carried out for assessing the noise locally and proposed adaptive soft thresholding is applied for suppressing noise. The denoised image in the first step further processed by Joint Bilateral Filter (JBL) [16] for removing noise residuals existing after the first step and producing visually appealing denoised image. The experimental results shows the superiority of the proposed method over state of art methods. Both qualitative and quantitative analysis shows the comparable performance of the algorithm.

The rest of the paper arranged as follows. The architecture of the proposed method discussed in the immediate section. The quantitative and qualitative analysis of the method discussed after the architecture of the method. The paper concluded in the last section.

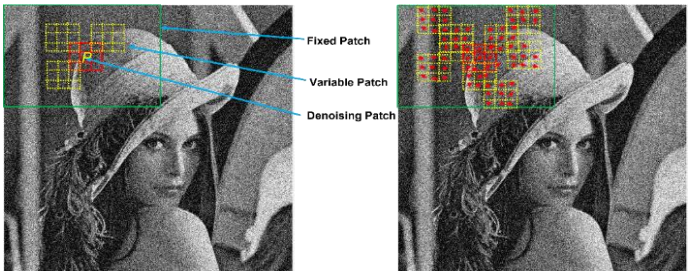

(a) (b)

Fig.2. Analysis of Patch Grouping and similarity in orientation (a) Illustration of patch selection (b) Orientation of pixels

2. PROPOSED METHOD

The proposed method removes noisy observation in two steps by incorporating PCA based noise suppression in transform domain and spatial domain based JBF. An ESI for patch grouping and a soft thresholding for noise suppression is proposed in this paper. The first step of the proposed algorithm works iteratively for each pixel of the image. For denoising a pixel, the pixel centered patch is identified and similar patches in its neighbourhood are grouped according to ESI. The similar patches are identified from the neighbourhood by the assumption that most similar patches will exists locally. The identification of optimal patches is the crucial steps of the algorithm. Inappropriate grouping of patches will lead to artifacts in denoised image and most of the indexing techniques exist in literature [13] is vulnerable to noise. The proposed ESI is an orientation-based index which group the patches with similar orientation. The optimal patches formed a stacked patch matrix and transformed in PCA domain where the noisy observations and noise free observation are easily distinguished. In PCA domain, the proposed adaptive soft thresholding method is applied for noise suppression. The thresholding parameter for each stacked patch matrix is identified by estimating noise level of patch matrix. The distribution of noise in a scene is different for different regions, hence global estimation of noise level does not work well. In proposed method each stacked patch matrix processed separately according to the concentration of noise present in it. The experimental results show the advantage of adaptive method for noise suppression. Noise residuals may exist after first step if the presence of noise is high. Hence in proposed method the denoised image again processed in spatial domain by JBF. The JBF is the improvement of the Bilateral filter [17], which is the most commonly used denoising filter in literature. The Bilateral filter give more weightage to the pixels which have same intensity of centre pixel and both spatially and radiometrically near to it. The drawback of classic Bilateral filter is that it is accurate to estimate the stepping function in the presence of noise and results in salt noise residuals. The architecture of the proposed method is shown in Fig.1. The steps for selecting optimal patches are described in the following section.

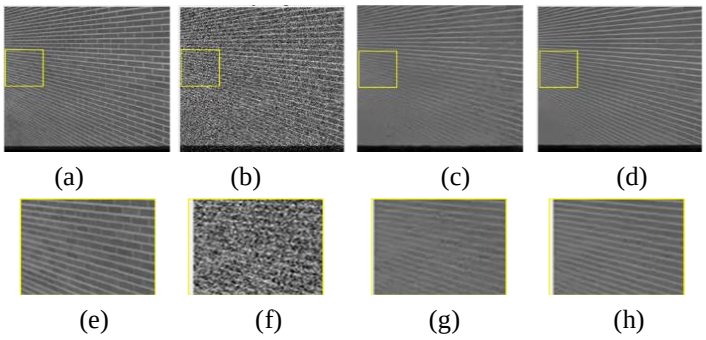

(a) (b) (c) (d)

(e) (f) (g) (h)

Fig.3(a). Original image (b)Noisy image with noise level σ=45 (c) Denoised image after the first step of the proposed (PSNR=27.18) (d) Denoised image after the second step of the proposed method (PSNR=29.18) (e) Enlargement of marked region of (a) (f) Enlargement of marked region of (b) (g) Enlargement of marked region of (c) (h) Enlargement of marked region of (d)

2.1 ESI BASED PATCH GROUPING

Let I_n be the noisy image contaminated by Gaussian Noise with zero mean and standard deviation σ. As noise is uncorrelated from pixel, the noisy pixel, y, of the image can be denoted as:

$$y=x+n \quad (1)$$

where x is the noise free pixel and n is the noise which follows the Gaussian distribution. For denoising the pixel, y, a set of

overlapping patches are identified from its neighbourhood. As shown in Fig.2(a), a Denoising patch centered on *y*, of size $n\times n$ is identified from a Fixed patch of size $m\times m$, where $n\leq m$, as described in [13]. In total $(m\text{-}n+1)$-number of overlapping optimal patches referred as Variable patch of size, $n\times n$ are selected from Fixed Patch. Among the Variable patches the patches which are more similar to Denoising patch are computed using the proposed ESI index.

The most crucial part of the algorithm is to select the most optimal patches among set of Variable patches. election of all Variable patches for denoising process will lead to inaccurate estimation of covariance matrix in PCA domain and results in unfruitful denoising. For selecting most optimal patches for denoising, several techniques exist in literature. The patches can be classified in two groups based on a clustering problem or block matching. The correlation between the patches is also used as similarity measure in literature. In proposed algorithm, an ESI which give more emphasise to details feature are proposed. The ESI measure the similarity in the detail of the patches for finding optimal variable patches. Since the detail will be affected less by the noise, similar patches can be identified accurately. ESI measures the similarity between patches in terms of its orientation instead of magnitude and, the ESI is higher if two patches have same orientation. The identified orientation for each pixel in the patches is shown in Fig.2(b).

(a) (b) (c) (d) (e) (f)

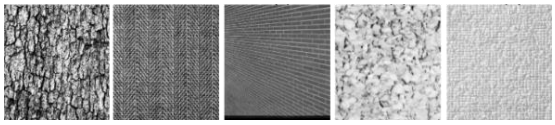

(g) (h) (i) (j) (k)

Fig.4 Test Images (a) Barbara (b) Boat (c) Bridge (d) Cameraman (e) Lena (f) Man (g) Texture1 (h) Texture2 (i) Texture3 (j) Texture4 (k) Texture5

Let $\vec{y}_r$ be the central column vector patch, which contain the pixel *y*, in the stacked patch matrix referred as reference column vector. The reference column vector consists of all the pixel in the Denoising patch. Let $\vec{y}_i$ be the i^{th} column vector patch where $i=\{1,2,3,\ldots,(m+n+1)^2\}$ be the other column vectors consists of the pixels of corresponding variable patches.

The Edge Similarity Index of i^{th} patch vector is defined as:

$$ESI_i = \frac{\vec{y}_r^t \vec{y}_i}{\|\vec{y}_r\|\|\vec{y}_i\|} \tag{2}$$

where $\vec{y}_r^t$ be the transpose of $\vec{y}_r$.

Let $\|\vec{y}_r\|$ and $\|\vec{y}_i\|$ defined as:

$$\|\vec{y}_r\| = \sqrt{\vec{y}_{r_1}^2 + \vec{y}_{r_2}^2 + \ldots + \vec{y}_{r_{n^2}}^2} \tag{3}$$

$$\|\vec{y}_i\| = \sqrt{\vec{y}_{i_1}^2 + \vec{y}_{i_2}^2 + \ldots + \vec{y}_{i_{n^2}}^2} \tag{4}$$

where n^2 is the total pixels in each patch vector. The patch vector $\|\vec{y}_i\|$ selected as an optimal patch vector if:

$$ESI_i<£ \tag{5}$$

where £ is the preset threshold and experimentally £ set as 25.

Let *p* number of patch vectors selected as optimal patch vectors, then the dataset of optimal patch vector defined as:

$$Y = \left[\vec{y}_0, \vec{y}_1, \ldots, \vec{y}_p\right] \tag{6}$$

Corresponding noiseless optimal patch vectors denoted as:

$$X = \left[\vec{x}_0, \vec{x}_1, \ldots, \vec{x}_p\right] \tag{7}$$

where *p* set as $c.m$ and the for better representation of patch in PCA domain, the constant *c* assigned the value between 8 to 10 by experiment.

The selected optimal sample patch vectors, *Y* are transformed into PCA domain where noise is suppressed, and noiseless sample patch *X* is estimated. The estimated patch *X* can replace the noise patch *Y* and algorithm can be applied iteratively to next pixel. The proposed noise suppression method described in the following section.

2.2 IMAGE DENOISING IN PCA DOMAIN

The advantage of denoising in PCA domain is that noise and signal are distinguished in such a way that the energy will become concentrated on small subset. The stacked patch matrix with optimal sample patches is transformed in PCA domain where noisy observations are suppressed using the proposed adaptive soft thresholding based on the local noise estimation. The global noise estimation failed to estimate the noise efficiently for each region as noise affected differently over regions of a scene. We modified the algorithm proposed in [14] and used for estimating noise at local level based on local statistics of the image.

Let *Y* represent the $m\times n$ stacked patch matrix, and the relationship between noiseless counterpart *X* and noisy observation *Y* is defined as:

$$Y=X+U \tag{8}$$

where *U* represent the observations affected by the additive Gaussian noise and is uncorrelated from *X*.

The *m* rows of stacked patch matrix, *Y* denoted as $Y = \left[Y_1^T, \ldots, Y_m^T\right]$ where Y_i, be the row vector which contains n samples of y_i. Similarly noiseless observations *X* and noise counterpart *U* can be denoted as $X = \left[X_1^T, \ldots, X_m^T\right]$ and $U = \left[U_1^T, \ldots, U_m^T\right]$ respectively. The dataset *Y* can be centralized as $\bar{Y}_i = Y_i - \mu_i$ where $\mu_i = \frac{1}{n}\sum_{j=1}^{n} Y_i(j)$. Since the mean value of additive noise is zero, the noisy observation dataset *X* can be centralized as $\bar{X}_i = Y_i - \mu_i$. The PCA transformation matrix $P_{\bar{X}}$ can be computed by calculating the covariance matrix $\Omega_{\bar{X}}$ of $\bar{X}$. Since $\bar{X}$ is unknown, $\Omega_{\bar{X}}$ can be estimated from the covariance matrix $\Omega_{\bar{Y}}$ of $\bar{Y}$ as described in [13]. PCA base can be obtained from the Singular Value Decomposition (SVD) of $\Omega_{\bar{Y}}$ and represented as:

$$\Omega_{\bar{Y}} = \frac{1}{n}\bar{Y}\bar{Y}^T = \frac{1}{n}\left(\bar{X}\bar{X}^T + \bar{X}U^T + U\bar{X}^T + UU^T\right) \quad (9)$$

As $\bar{X}$ and U are uncorrelated the terms $\bar{X}U^T$ and $U\bar{X}^T$ become zero and can be eliminated. Then $\Omega_{\bar{Y}}$ becomes:

$$\Omega_{\bar{Y}} = \frac{1}{n}\left(\bar{X}\bar{X}^T + UU^T\right) = \Omega_{\bar{X}} + \Omega_U \quad (10)$$

Expressing $\Omega_{\bar{Y}}$ in terms of eigen vectors and eigen values denoted as:

$$\Omega_{\bar{Y}} = \Phi_{\bar{Y}}\Lambda_{\bar{Y}}\Phi_{\bar{Y}}^T \quad (11)$$

The orthonormal PCA transformation matrix of $\bar{Y}$ can be set as:

$$P_{\bar{Y}} = \Phi_{\bar{Y}}^T \quad (12)$$

Applying $P_{\bar{Y}}$ to dataset $\bar{Y}$, we have:

$$\bar{\bar{Y}} = P_{\bar{Y}}\bar{Y} = P_{\bar{Y}}\left(\bar{X} + \bar{U}\right) = P_{\bar{Y}}\bar{X} + P_{\bar{Y}}\bar{U} = \bar{X} + \bar{U} \quad (13)$$

Most important component in $\bar{\bar{Y}}$ represent the noiseless dataset $\bar{\bar{X}}$ and least important component represent $\bar{U}$. As σ^2 is the standard deviation of the noisy matrix $\bar{U}$, the noise level σ can be directly estimated from eigen values, λ_U of $\bar{U}$. Here $\bar{U}$ is unknown and noisy observations are evenly distributed in $\bar{\bar{Y}}$. According to [14], the eigen values of $\bar{\bar{Y}}$ and eigne values of $\bar{X}$ are same and hence , λ_U can be estimated from eigne vectors, $\Phi_{\bar{Y}}$ of $\bar{\bar{Y}}$. Hence, noise level for the patch can be estimated from the eigne vectors of $\bar{\bar{Y}}$. The noise level for the stacked patch matrix can be computed using the following equations:

$$\sigma^2 = E\left(\lambda_U\right) \approx \frac{\sum_{i=1}^{M}\lambda_Y U\left(\lambda_{U^-}, \Phi_{\bar{Y}_m}, \lambda_{U^+}\right)}{\sum_{i=1}^{M} U\left(\lambda_{U^-}, \Phi_{\bar{Y}_m}, \lambda_{U^+}\right) + \varepsilon} \quad (14)$$

$$\sigma^2 = \frac{\lambda_{U^-} + \lambda_{U^+}}{4\sqrt{\gamma}} \quad (15)$$

where $\gamma=m/n$ and $\lambda_{U^-} = \Phi_{\bar{Y}_m}$ and

$$U = \begin{cases} 1 & if\ \lambda_{U^-} \le \Phi_{\bar{Y}_m} \le \lambda_{U^+} \\ 0 & otherwise \end{cases} \quad (16)$$

For computing λ_{U^+}, the difference Δi is calculated:

$$\Delta_i = \left\|\sigma_{i1}^2 - \sigma_{i2}^2\right\|_2^2 \quad (17)$$

where σ_{i1}^2 computed according to Eq.(14) and σ_{i2}^2 according to Eq.(15) and λ_{U^+} assign the value of $\Phi_{\bar{Y}_i}$, $1 \le i \le m$ and the value of $\Phi_{\bar{Y}_i}$ which minimize Eq.(17) set as λ_{U^+}. The noise level σ is computed by applying this value to λ_{U^+} in Eq.(14).

Let $g_{i,j}$ be the noisy observations in $\bar{\bar{Y}}$. The spatially adaptive soft thresholding for this patch is defined as

$$T = \frac{\sigma_g^2}{\sigma^2} \quad (18)$$

where $\sigma_g^2 = \max\left(\frac{1}{2k+1}\sum_g g_{i,j}^2 - \sigma^2, 0\right)$

The estimated noise power σ^2 needs to be subtracted from the noisy observations. The soft threshold for each Y is calculated and noise is supressed. The method performed for all pixels in the image and produces the denoised image

2.3 DENOISING BY JOINT BILATERAL FILTER

The denoised image from first step is further processed in spatial domain by JBF for removing noise residuals exist after first step. JBF. The presence of strong noise results errors in selection of optimal patches and results estimation bias in PCA transformation. Hence, performance of denoising algorithm has affected. A further processing of denoised result is required for producing a visually pleasing denoised image.

Let $\hat{I}$ be the denoised image from first step and $s_{i,j}$ be the pixel at the location (i,j) in $\hat{I}$. The corresponding denoised pixel $\hat{S}_{i,j}$ defined as

$$\tilde{S}_{i,j} = \frac{\sum_{a,b\in\omega} h_{La,b}h_{Ea,b}u_{a,b}}{\sum_{a,b\in\omega} h_{La,b}h_{Ea,b}} - \mu\rho_{i,j} \quad (19)$$

where $u_{i,j}$ be the noisy observation in location (i,j) the image I and ω is the window of size $n\times n$ and h_L and h_E are low pass filter and edge stopping function respectively. The edge stopping function defined as:

$$h_{Ea,b} = \exp\left[\frac{-\left|s_{a,b}^{ref} - s_{i,j}^{ref}\right|}{\delta_E}\right] \quad (20)$$

where S^{ref} is the denoised reference image and δ_E is the smoothing function. Let Low pass filter $h_{La,b}$ defined as:

$$h_{La,b} = \exp\left[\frac{-(a-i)^2 + (b-j)^2}{2\delta_E^2}\right] \quad (21)$$

and μ=[0,1] and $\rho_{i,j} = \frac{\sum_{a,b\in\omega} h_{La,b}h_{Ea,b}\left(u_{a,b} - s_{a,b}^{ref}\right)}{\sum_{a,b\in\omega} h_{La,b}h_{Ea,b}}$

Experimental results shows that the best value for $\mu\in$[0.6,0.8] and $\delta_E\in$[3,12]. The Fig.3 illustrates the requirement of second stage for denoising. As shown in Fig.3(c) and Fig.3(d) the image quality and PSNR improved in the second step.

Table.1. PSNR (dB) results of the denoised images at different noise levels and by different schemes

Method	**BM3D**	**LPG-PCA**	**WN-NM**	**SLRD**	**WT-RD**	**Prop.**	**BM3D**	**LPG-PCA**	**WN-NM**	**SLRD**	**WT-RD**	**Prop.**
σ	**15**						**45**					
Barbara	31.82	32.14	32.89	32.81	32.89	33.01	26.19	25.98	27.55	27.27	27.23	28.50
Boat	31.62	30.67	31.43	31.47	31.54	31.83	26.58	25.03	25.99	26.02	26.15	27.36
Bridge	28.12	28.55	26.76	28.96	26.65	29.15	23.60	23.41	24.02	23.97	23.99	23.64
Cameraman	31.38	31.99	31.99	32.01	32.02	32.06	26.14	26.75	26.80	26.99	26.82	31.74
Lena	32.17	32.35	33.02	33.03	33.08	33.10	26.32	26.46	27.49	27.63	27.58	27.18
Man	29.65	29.84	30.45	30.53	30.47	30.86	24.52	24.36	25.16	25.32	25.16	24.86
Texture 1	25.60	26.03	26.18	26.22	26.19	26.90	18.65	19.02	19.42	19.45	19.46	17.61
Texture 2	26.79	27.02	25.78	27.38	27.38	28.10	20.35	20.16	21.94	22.06	22.06	21.31
Texture 3	32.43	32.36	33.20	32.88	33.29	31.23	25.95	26.08	29.00	29.33	28.81	29.18
Texture 4	30.45	30.88	31.42	31.37	31.44	31.04	24.20	24.26	25.39	25.34	25.32	24.96
Texture 5	29.33	29.32	30.18	30.26	30.16	30.20	24.09	24.04	24.75	24.46	24.64	25.23
Average	**29.94**	**30.10**	**30.30**	**30.63**	**30.46**	**30.68**	**24.24**	**24.14**	**25.23**	**25.26**	**25.20**	**25.60**
σ	**75**						**90**					
Barbara	23.55	23.22	24.35	24.88	24.81	25.02	22.67	22.28	23.54	24.00	24.06	24.26
Boat	23.00	22.87	23.87	23.96	23.92	24.62	22.30	22.17	22.74	22.65	23.77	24.07
Bridge	21.81	21.52	23.05	22.32	22.93	22.83	21.16	20.89	21.46	21.77	21.73	21.85
Cameraman	23.58	24.25	24.51	24.78	24.69	24.91	22.65	23.37	23.33	24.02	24.08	24.18
Lena	22.87	23.92	25.21	25.38	25.40	25.41	23.12	23.03	24.01	24.63	24.37	24.27
Man	22.31	22.11	23.09	23.28	23.11	23.50	21.56	21.36	22.00	22.56	22.54	22.74
Texture 1	16.36	16.34	16.06	17.07	17.08	16.44	15.63	15.56	15.93	16.32	16.34	16.14
Texture 2	17.46	23.57	19.89	20.12	20.03	20.55	16.75	16.99	18.49	19.87	19.45	19.53
Texture 3	23.29	23.32	26.66	26.41	26.39	26.89	22.69	22.92	24.43	24.24	24.27	24.87
Texture 4	21.65	21.63	22.90	22.74	22.78	22.69	20.85	20.82	22.00	21.86	21.93	22.03
Texture 5	22.90	22.91	22.80	22.67	22.45	23.35	22.58	22.68	22.45	22.38	22.44	21.78
Average	**21.71**	**22.33**	**22.94**	**23.06**	**23.05**	**23.29**	**21.09**	**21.10**	**21.85**	**22.21**	**22.27**	**22.34**

Table.2. EPI results of the denoised images at different noise levels and by different schemes.

Method	**BM3D**	**LPG-PCA**	**WN-NM**	**SLRD**	**WT-RD**	**Prop.**	**BM3D**	**LPG-PCA**	**WN-NM**	**SLRD**	**WT-RD**	**Prop.**
σ	**15**						**45**					
Barbara	0.88	0.90	0.91	0.92	0.81	0.97	0.66	0.71	0.73	0.79	0.60	0.75
Boat	0.84	0.87	0.89	0.88	0.81	0.88	0.68	0.67	0.70	0.71	0.50	0.72
Bridge	0.80	0.82	0.82	0.81	0.81	0.88	0.58	0.58	0.59	0.60	0.50	0.56
Cameraman	0.95	0.90	0.92	0.92	0.52	0.95	0.76	0.77	0.79	0.80	0.35	0.76
Lena	0.88	0.88	0.90	0.92	0.73	0.96	0.69	0.68	0.73	0.82	0.56	0.78
Man	0.84	0.84	0.86	0.87	0.75	0.95	0.60	0.61	0.64	0.70	0.51	0.77
Texture 1	0.91	0.92	0.92	0.96	0.96	0.92	0.67	0.70	0.69	0.82	0.82	0.84
Texture 2	0.92	0.92	0.90	0.97	0.97	0.95	0.75	0.76	0.80	0.87	0.88	0.88
Texture 3	0.93	0.92	0.94	0.95	0.93	0.99	0.67	0.74	0.85	0.89	0.83	0.88
Texture 4	0.91	0.92	0.93	0.91	0.85	0.95	0.78	0.81	0.80	0.76	0.64	0.74
Texture 5	0.87	0.87	0.88	0.88	0.87	0.90	0.73	0.75	0.76	0.51	0.45	0.79
Average	**0.88**	**0.89**	**0.90**	**0.91**	**0.82**	**0.94**	**0.69**	**0.71**	**0.74**	**0.75**	**0.60**	**0.77**
σ	**75**						**90**					
Barbara	0.51	0.58	0.62	0.70	0.49	0.65	0.45	0.54	0.59	0.67	0.46	0.60

Boat	0.49	0.54	0.59	0.63	0.36	0.65	0.44	0.50	0.53	0.59	0.30	0.61
Bridge	0.44	0.47	0.49	0.49	0.37	0.47	0.39	0.44	0.49	0.45	0.33	0.47
Cameraman	0.60	0.65	0.68	0.75	0.26	0.76	0.53	0.60	0.62	0.73	0.24	0.64
Lena	0.57	0.56	0.61	0.75	0.47	0.64	0.52	0.51	0.55	0.72	0.41	0.63
Man	0.43	0.48	0.52	0.60	0.39	0.60	0.37	0.43	0.45	0.56	0.35	0.59
Texture 1	0.51	0.54	0.54	0.68	0.69	0.67	0.44	0.48	0.45	0.62	0.63	0.60
Texture 2	0.54	0.63	0.72	0.78	0.79	0.82	0.45	0.56	0.66	0.70	0.75	0.78
Texture 3	0.41	0.52	0.73	0.72	0.64	0.76	0.33	0.43	0.55	0.51	0.40	0.72
Texture 4	0.70	0.75	0.77	0.62	0.47	0.60	0.66	0.73	0.75	0.56	0.42	0.60
Texture 5	0.66	0.71	0.70	0.25	0.08	0.70	0.63	0.69	0.68	0.22	0.25	0.61
Average	**0.53**	**0.58**	**0.64**	**0.63**	**0.46**	**0.66**	**0.47**	**0.54**	**0.57**	**0.58**	**0.41**	**0.62**

Fig.5(a). Boat image, (aa) Image corrupted by Gaussian noise, σ=15, (ba) Image corrupted by Gaussian noise, σ=45, (ca) Image corrupted by Gaussian noise, σ=75, (ab-cb) Image restored using BM3D from (aa-ca), (ac-cc) Image restored using LPG-PCA from (aa-ca), (ad-cd) Image restored using the WNNM from (aa-ca), (ae-ce) Image restored using the SLRD from (aa-ca) (af-cf) Image restored using the WTRD from (aa-ca) (ag-cg) Image restored using the Proposed method from (aa-ca)

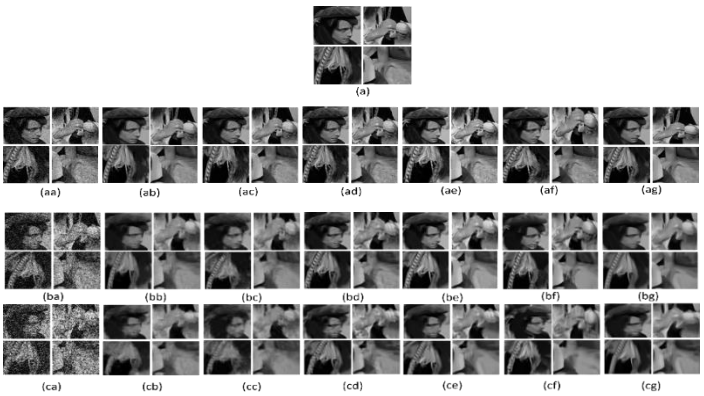

Fig.6(a). Man image, (aa) Image corrupted by Gaussian noise, σ=15, (ba) Image corrupted by Gaussian noise, σ=45, (ca) Image corrupted by Gaussian noise, σ=75, (ab-cb) Image restored using BM3D from (aa-ca), (ac-cc) Image restored using LPG-PCA from (aa-ca), (ad-cd) Image restored using the WNNM from (aa-ca), (ae-ce) Image restored using the SLRD from (aa-ca) (af-cf) Image restored using the WTRD from (aa-ca) (ag-cg) Image restored using the Proposed method from (aa-ca)

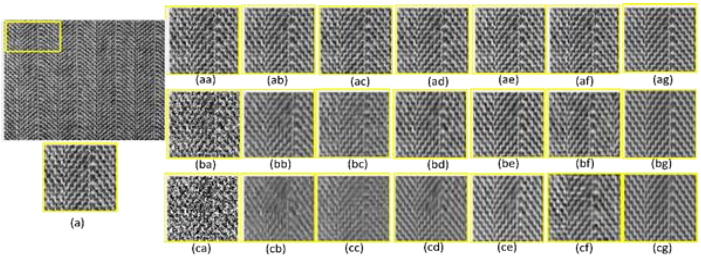

Fig.7(a). Texture1 image, (aa) Image corrupted by Gaussian noise, σ=15, (ba) Image corrupted by Gaussian noise, σ=45, (ca) Image corrupted by Gaussian noise, σ=75, (ab-cb) Image restored using BM3D from (aa-ca), (ac-cc) Image restored using LPG-PCA from (aa-ca), (ad-cd) Image restored using the WNNM from (aa-ca), (ae-ce) Image restored using the SLRD from (aa-ca) (af-cf) Image restored using the WTRD from (aa-ca) (ag-cg) Image restored using the Proposed method from (aa-ca)

3. RESULTS AND DISCUSSION

This section compares the denoising performance of proposed algorithm with state-of-the-art denoising algorithms. Fig.4 shows the test images for analyzing the algorithms and consist of standard images and texture images [18]. The proposed algorithm evaluated with the benchmark images at various Gaussian levels ranging from 15 to 90 as done in other papers. The recently developed algorithm BM3D [6], LPG-PCA [13], SLRD [19], WNNM [20], and WTRD [21], are used for comparing performance of the proposed algorithm.

The experimental results of four images at various noise levels are shown in Fig.5–Fig.7 for visual analysis. For quantitative analysis, Peak Signal-to-Noise Ratio (PSNR) and Edge preservation index (EPI) [22] are used as performance measures. The PSNR and EPI values are calculated for all benchmark images at various noise levels for proposed method and existing algorithms. By comparing visual analysis and quantitative analysis the proposed method outperforms all existing denoising algorithms.

In the implementation level of proposed method, a noise free pixel is obtained by average value of all optimal Variable patches in its Fixed patch. The size of variable patch set as 5 and Fixed patch as 40 by experiment. Default parameters in author's paper is used for the state-of-the-art algorithms for getting the best result for comparison. The gaussian white noise at various levels 15, 45, 75 and 90 are added to the benchmark images and denoising performance of the methods are compared using the source code obtained from author website. The algorithms compared over 10 benchmark images which consists of 5 standard images and 5 texture images [18]. For visual analysis partial results are included in the paper due to shortage of space. The result of quantitative analysis of 10 image for all noise level are include in the paper.

3.1 VISUAL ANALYSIS

The visual pleasantness of denoised image of the proposed algorithm over other competing algorithms are illustrated in Fig.5 to Fig.7. The noise contamination at low, moderate and high level on 'boat' image shown in Fig.5(aa) - Fig.5(ca) respectively. The enlarged portions of the image shown the denoising performance of algorithms in edges and flat regions. The visual inspection reveals the outstanding performance of the proposed method over the comparing methods. For the noise level σ=15, the name board in the boat, as shown in Fig.5(ag), is completely recovered by the proposed method than other method.

Although BM3D algorithm retains the sharp structures as demonstrated in Fig.5(ab)- Fig.5(cb), it fails to restore the smooth regions. The denoised images of the method LPG-PCA, WNNM, SLRD and WTRD shown in Fig.5(ac)-Fig.5(cc), Fig.5(ad)-Fig.5(cd), Fig.5(ae)-Fig.5(ce), and Fig.5(af)-Fig.5(cf), respectively demonstrate that flat areas are blurred and name plate of boat is not restored completely. In Fig.6 the cropped regions of man image are displayed for more visibility of the denoising performance of the algorithms. The denoised image of the methods LPG-PCA, WNNM, SLRD and WTRD in Fig.6(ac)-Fig.6(cc), Fig.6(ad)-Fig.6(cd), Fig.6(ae)-Fig.6(ce), and Fig.6(af)-Fig.6(cf) respectively, shows that artifacts are generated over the forehead of the man image and, the sharp regions are blurred. Although BM3D performs well in comparing to other methods, the proposed method produces more visually pleasant denoised image as shown in Fig.6(ag)-Fig.6(cg) for all noise levels. For higher levels of noise, the performance of the proposed methods was comparable result over other state of art algorithms.

The Fig.7 is the texture image used for comparing the texture restoring capability of the denoising algorithm. The marked portions of the images shown in Fig.7(a) has zoomed for comparison of competing methods with proposed method. For moderate noise level, σ=45, as illustrated in Fig.7(bb)-Fig.7(bg), the competing method blurs the texture and distort their structures. In high noise level, the better performance of proposed method is shown in Fig.8(cg) over other methods as illustrated in Fig.7(cb)-Fig.7(cf). The visual analysis reveals the outstanding performance of the proposed method at different noise levels.

3.2 QUANTITATIVE ANALYSIS

The superiority of proposed method over other methods are shown in the value of PSNR and EPI of benchmark images. The PSNR value of all images at different noise levels are reported in Table.1. Although SLRD have the mean PSNR value of 30.63, 25.26 and 23.06 for noise level 15, 45 and 75 respectively, the proposed method achieves the first position. The edge preserving capability of the proposed method is compared with other algorithm by analysing EPI values. While comparing values of EPI, the EPI values of proposed method is better than all other algorithms as shown in Table.2. Even though, both WNMM and SLRD performs well for preserving edges, both fails to produce a visually appealing result and artifacts are generated.

4. CONCLUSIONS

A two-step denoising algorithm has been proposed in order to solve the drawbacks of the existing methods. The advantage of both transform domain and spatial domain filtering are utilized in proposed algorithm for removing noise components. In the first step the optimal patches for denoising are identified using proposed Edge Similarity Index (ESI) and transferred to PCA domain where noise estimation and noise suppression is performed. The local noise estimation helps to estimate the noise accurately and proposed adaptive soft thresholding separates the noisy observations from noisy observations. The noise component present after first step is denoised by the Joint Bilateral Filter in spatial domain. The proposed method shown its better performance in visual analysis and quantitative analysis. The superiority of the method over other state of art method is shown in the value of Peak Signal-to-Noise Ratio (PSNR) and Edge preservation index (EPI). In future, this work can be improved by finding more adaptive indexing for identifying optimal patches and thus, improve the detail preserving capability of the algorithm.

REFERENCES

[1] C. Tomasi and R. Manduchi, "Bilateral Filtering for Gray and Color Images", *Proceedings of IEEE International Conference on Computer Vision*, pp. 839-846, 1998.

[2] P. Perona and J. Malik, "Scale-Space and Edge Detection using Anisotropic Diffusion", *IEEE Transactions on Pattern Analysis and Machine Intelligence*, Vol. 12, pp. 629-639, 1990.

[3] H. Takeda, S. Farsiu and P. Milanfar, "Kernel regression for Image Processing and Reconstruction", *IEEE Transactions on Image Processing*, Vol. 16, No. 2, pp. 349-366, 2007.

[4] A. Buades, B. Coll and J. Morel, "A Non-Local Algorithm for Image Denoising", *Proceedings of IEEE International Conference on Computer Vision and Pattern Recognition*, pp. 1-12, 2005.

[5] V. Katkovnik, A. Foi, K. Egiazarian and J. Astola, "From Local Kernel to Nonlocal Multiple-Model Image Denoising", *International Journal on Computer Vision*, Vol. 86, No. 1, pp. 1-32, 2010.

[6] K. Dabov, A. Foi, V. Katkovnik and K. Egiazarian, "Image Denoising by Sparse 3D Transform-Domain Collaborative Filtering", *IEEE Transactions on Image Processing*, Vol. 16, No. 8, pp. 2080-2095, 2007.

[7] L.Z. Manor, K. Rosenblum and Y.C. Eldar, "Dictionary Optimization for Block-Sparse Representations", *IEEE Transactions on Signal Processing*, Vol. 60, No.5, pp. 2386-2395, 2012.

[8] P. Chatterjee and P. Milanfar, "Patch-Based Near-Optimal Image Denoising", *IEEE Transactions on Image Processing*, Vol. 21, No. 4, pp. 1635-1649, 2012.

[9] Y. Ding and I.W. Selesnick, "Artifact-Free Wavelet Denoising: Non-Convex Sparse Regularization, Convex Optimization", *IEEE Transactions on Signal Processing Letters*, Vol. 22, No. 9, pp. 1364-1368, 2015.

[10] A.E. Cetin and M. Tofighi, "Projection-Based Wavelet Denoising", *IEEE Signal Processing Magazine*, Vol. 32, No. 5, pp. 120-124, 2015.

[11] Sergey Krivenko, Vladimir Lukin, Benoit Vozel and Kacem Chehdi, "Prediction of DCT-Based Denoising Efficiency for Images Corrupted by Signal-Dependent Noise", *Proceedings of IEEE 34th International Scientific Conference on Electronics and Nanotechnology*, pp. 1-12, 2014.

[12] K. Fukunaga, "*Introduction to Statistical Pattern Recognition*", 2nd Edition, Academic Press, 1991.

[13] L. Zhang,W. Dong, D. Zhang and G. Shi, "Two-Stage Image Denoising by Principal Component Analysis with Local Pixel Grouping", *Pattern Recognition*, Vol. 43, No. 4, pp. 1531-1549, 2010.

[14] Wenzhao Zhao, Yisong Lv, Qiegen Liu and Binjie Qin, "Detail-Preserving Image Denoising Via Adaptive Clustering and Progressive PCA Thresholding", *IEEE Access*, Vol. 6, pp. 6303-6315, 2018.

[15] D.D. Muresan and T.W. Parks, "Adaptive Principal Components and Image Denoising", *Proceedings of International Conference on Image Processing*, Vol. 1, pp. 101-104, 2003.

[16] Hancheng Yu, Li Zhao and Haixian Wang, "Image Denoising using Trivariate Shrinkage Filter in the Wavelet Domain and Joint Bilateral Filter in the Spatial Domain", *IEEE Transactions on Image Processing*, Vol. 18, No. 10, pp. 2364-2369, 2009.

[17] C. Tomasi and R. Manduchi, "Bilateral Filtering for Gray and Color Images", *Proceedings of International Conference on Computer Vision*, pp. 839-846, 1998.

[18] T. Randen. "Brodatz Textures", Available at: http://www.ux.uis.no/~tranden/brodatz.html, Accessed at 2007.

[19] Mansour Nejati, Shadrokh Samavi, Harm Derksen and Kayvan Najarian, "Denoising by Low-Rank and Sparse Representations", *Journal of Visual Communication and Image Representation*, Vol. 36, pp. 28-39, 2016.

[20] Shuhang Gu, Lei Zhang, Wangmeng Zuo and Xiangchu Feng, "Weighted Nuclear Norm Minimization with Application to Image Denoising", *Proceedings of IEEE Conference on Computer Vision and Pattern Recognition*, pp. 2862-2869, 2014.

[21] Y. Wu, L. Fang and S. Li. "Weighted Tensor Rank-1 Decomposition for Nonlocal Image Denoising", *IEEE Transactions on Image Processing*, Vol. 28 No. 6, pp. 2719-2730, 2019.

[22] F. Sattar, L. Floreby, G. Salomonsson and B. "Lovstrom. Image Enhancement based on a Nonlinear Multiscale Method", *IEEE Transactions on Image Processing*, Vol. 6, No. 6, pp. 888-895, 1997.